Taming the Signal-to-Noise Problem in Lattice QCD by Phase Reweighting

Michael L. Wagman[1, 2] and Martin J. Savage[1, 2]

(NPLQCD Collaboration)

[1]*Institute for Nuclear Theory, University of Washington, Seattle, WA 98195-1550, USA*
[2]*Department of Physics, University of Washington, Box 351560, Seattle, WA 98195, USA*
(Dated: July 12, 2017)

Path integrals describing quantum many-body systems can be calculated with Monte Carlo sampling techniques, but average quantities are often subject to signal-to-noise ratios that degrade exponentially with time. A phase-reweighting technique inspired by recent observations of random walk statistics in correlation functions is proposed that allows energy levels to be extracted from late-time correlation functions with time-independent signal-to-noise ratios. Phase reweighting effectively includes dynamical refinement of source magnitudes but introduces a bias associated with the phase. This bias can be removed by performing an extrapolation, but at the expense of re-introducing a signal-to-noise problem. Lattice Quantum Chromodynamics calculations of the ρ^+ and nucleon masses and of the $\Xi\Xi(^1S_0)$ binding energy show consistency between standard results obtained using earlier-time correlation functions and phase-reweighted results using late-time correlation functions inaccessible to standard statistical analysis methods.

The signal-to-noise (StN) problem inherent to Monte Carlo sampling of quantum mechanical correlation functions provides a substantial impediment to precision calculations of multi-particle systems across many areas of physics, from Lattice Quantum Chromodynamics (LQCD) and nuclear many-body calculations to calculations of the properties of materials. In LQCD, where the quantum fields responsible for the strong and electromagnetic forces are sampled numerically on a discretized spacetime to calculate path integrals, the StN problem has restricted calculations to mesons, the nucleon, and the lightest few nuclei. Ideally, calculations of larger nuclei and of the dense matter present in the interior of neutron stars would also be performed directly with LQCD, but the StN problem provides a substantial roadblock.

StN problems in LQCD have been studied since the pioneering works of Parisi [1] and Lepage [2], and arises when there are states contributing to a variance correlation function with less than twice the energy of the ground state of the correlation function. Correlation functions describing one or more baryons in LQCD have exponentially degrading StN ratios at late (Euclidean) times, with the argument of the exponent increasing with the number of baryons [3]. The statistical distributions of correlation functions sampled in Monte Carlo calculations have interesting features [3–13], and in particular the logarithms of LQCD correlation functions exhibit characteristics of Lévy Flights associated with heavy-tailed Stable Distributions [14]. At early and intermediate times, the distribution of the real parts of nucleon correlation functions is asymmetric with odd moments

that fall exponentially with the nucleon mass, M_N, and, in contrast, even moments that fall exponentially with the pion mass, M_π [13]. This leads to a distribution at late times that is symmetric and non-Gaussian and a nucleon StN ratio proportional to $\sim e^{-(M_N-3M_\pi/2)t}$. Sink optimization for baryon and multi-baryon systems [3–5, 13, 15–18], and more sophisticated variational methods in the mesonic sector [19–22], can extend the plateau region where correlation functions achieve approximate ground-state saturation to earlier times. In this "golden window," variance correlation functions have not yet achieved ground-state saturation and StN degradation is exponentially less severe than at later times [3–5]. At very late times, nucleon correlation functions enter a noise region where standard statistical estimators, including the sample mean, become unreliable because of finite sample size effects associated with circular statistics [14].

To begin extracting meaningful results from the noise region, it is helpful to separately consider the magnitude and phase of nucleon correlation functions [14]. The average nucleon magnitude is observed to be proportional to $\sim e^{-3M_\pi t/2}$ at late times and does not exhibit a StN problem. In contrast, the average nucleon phase is observed to be proportional to $\sim e^{-(M_N-3M_\pi/2)t}$ at late times and has a severe StN problem. From this behavior, the StN problem in nucleon correlation functions was identified as a sign problem [14]. The sign problem encountered in estimating the phase of a correlation function is spacetime extensive and can be mitigated by restricting the time interval, Δt, over which the system contains specific con-
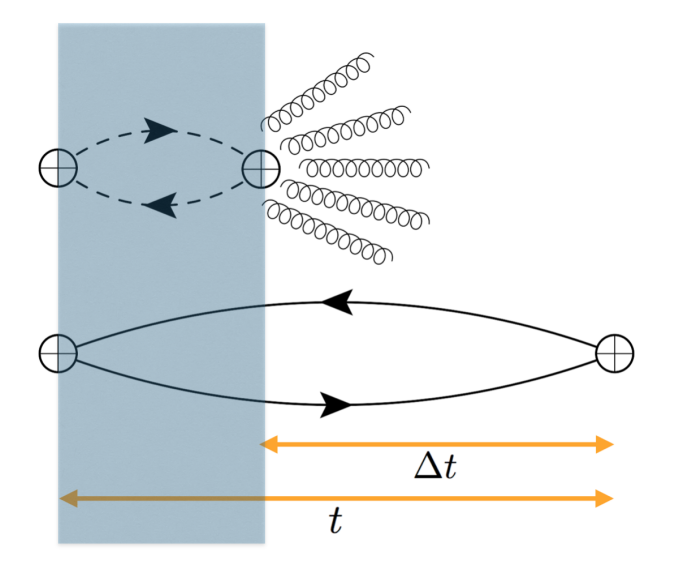
FIG. 1. The ρ^+-meson phase-reweighted correlation function $G^\theta_\rho(t, \Delta t)$ is a product of quark propagators forming $C^\rho_i(t)$, shown as solid lines, and a phase factor $e^{-i\theta^\rho_i(t-\Delta t)}$, shown as dashed propagator lines with reversed quark-charge arrows. Gluon lines indicate that phase reweighting introduces correlations associated with excitations produced at $t - \Delta t$ and lead to bias when $\Delta t \neq t$. For momentum-projected correlation functions, excitations involving correlated interactions between $C^\rho_i(t)$ and $e^{-i\theta^\rho_i(t-\Delta t)}$ are suppressed by the spatial volume. $G^\theta_\rho(t, \Delta t)$ effectively includes a non-local source whose magnitude is dynamically refined for $t-\Delta t$ steps while the phase is held fixed (shaded region) before the full system is evolved for the last Δt steps of propagation.

served charges prior to measurement. This restriction neglects correlations across distances larger than Δt and creates a bias in ground-state energies that decreases exponentially with increasing Δt.

This letter introduces a phase reweighting technique for LQCD correlation functions that allows ground-state energies to be extracted at late times with StN constant in t. By restricting the region where the complex phase associated with baryon number is allowed to evolve, phase reweighting makes Δt independent of t, but leads to a bias that must be systematically removed through extrapolation. The StN problem re-emerges as exponential loss of precision with increasing Δt.

Analogous techniques are used in applications of Green's Function Monte Carlo (GFMC) methods to nuclear many-body systems where the phase of the wavefunction is held fixed until the system is close to its ground state, at which point the phase is released for final evolution [23–26]. Similar techniques are also used in Lattice Effective Field Theory (LEFT) calculations in which a Wigner-symmetric Hamiltonian, emerging from the large-N_c limit of QCD [27], is used for initial time evolution before asymmetric perturbations are added that introduce a sign problem [28]. Phase reweighting shares

physical similarities, and possibly formal connections, to the approximate factorization of domain-decomposed quark propagators recently suggested and explored by Cè, Giusti and Schaefer [29–31].

LQCD calculations involve ensembles of a large number, N, of correlation functions $C_i(t)$, each calculated from a source on a particular gauge field configuration. Expectation values $G(t) = \langle C_i(t) \rangle$ can be computed from sample averages $G(t) = \frac{1}{N}\sum_i C_i(t)$ across field configurations importance sampled from the QCD vacuum probability distribution. The ground-state energy of correlation functions can be accurately determined from the late-time behavior of $G(t)$, but for generic correlation functions the StN problem restricts the extraction of precise ground-state energy measurements to early and intermediate times.

Phase reweighted correlation functions are defined by

$$G^\theta(t, \Delta t) = \langle e^{-i\theta_i(t-\Delta t)} \, C_i(t) \rangle \ , \qquad (1)$$

where $\theta_i(t - \Delta t) = \arg[C_i(t - \Delta t)]$. Phase reweighting resembles limiting the approximate Lévy Flight of the correlation function phase to Δt steps at late times, suggesting that $G^\theta(t, \Delta t)$ has a StN ratio that decreases exponentially with Δt but is constant in t. In the limit that $\Delta t \to t$, the reweighting factor approaches unity and $G^\theta(t, t) = G(t)$. The exact correspondence $G^\theta(t, t) = G(t)$ gives phase reweighting an advantage over our previously suggested estimator [14] involving multiplication by $C_i^{-1}(t - \Delta t)$ rather than $e^{-i\theta_i(t-\Delta t)}$. Phase reweighting also leads to more precise ground-state energy extractions than estimators involving reweighting with $C_i^{-1}(t-\Delta t)$; multiplication by the heavy-tailed variable $|C_i(t - \Delta t)^{-1}|$ leads to increases variance.

Dynamical correlations between $C_i(t)$ and $e^{-i\theta_i(t-\Delta t)}$ lead to differences in ground-state energies extracted from $G^\theta(t, \Delta t)$ and $G(t)$ for $t \neq \Delta t$. Locality suggests that these correlations should decrease exponentially with increasing Δt at a rate controlled by the longest correlation length in the theory. At asymptotically large Δt, one-pion-exchange correlations are expected to provide the largest contributions to the bias. These contributions will be suppressed by factors involving the spatial volume in products of a momentum-projected correlation function with a momentum-projected phase factor. Excitations involving the σ meson, correlated two-pion exchange, and other light excitations that do not change the quantum numbers of the system are not volume-suppressed and may dominate at small Δt. Near-threshold bound states may have complicated small Δt bias that is sensitive to the size of the spatial volume.

The construction of G^θ is generic for any correlation function, and is schematically depicted for the ρ^+ meson in Fig. 1. In the plateau region of the ρ^+ correlation function, the average of the magnitude is approximately pro-
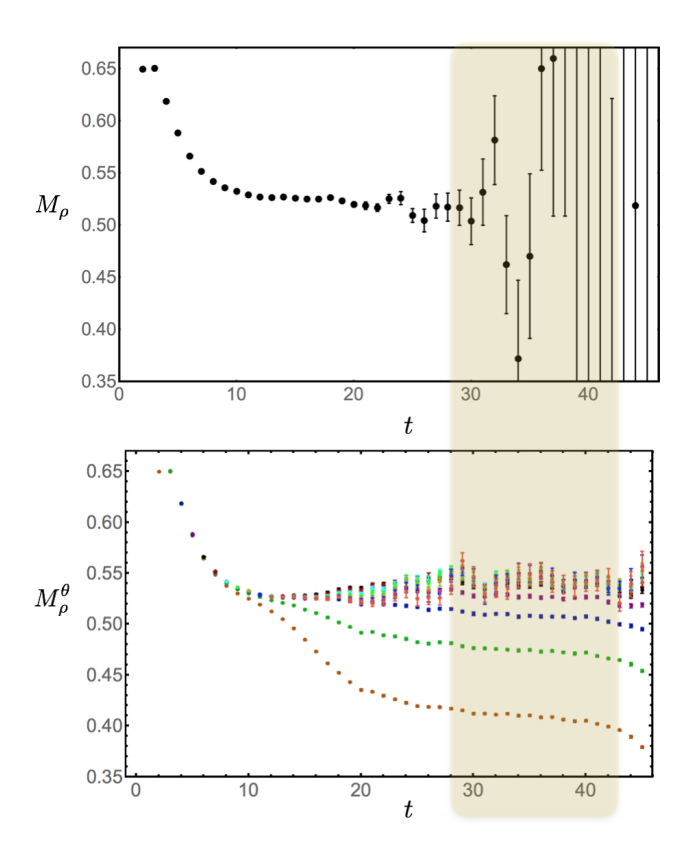
FIG. 2. The upper panel shows the ρ^+ effective mass from the LQCD ensemble of Ref. [32]. The lower panel shows $M_\rho^\theta(t, \Delta t)$ with a range of fixed Δt's. Temporal structure at later times arises from proximity to the midpoint of the lattice at $t = 48$. The highlighted interval $t = 28 \to 43$ is used for correlated χ^2 minimization fits of M_ρ^θ. Masses and times are given in lattice units.

portional to $e^{-M_\pi t}$, while the average of the phase factor[1] is approximately proportional to $e^{-(M_\rho - M_\pi)t}$. $G^\theta(t, \Delta t)$ is a product of these two averages plus corrections arising from correlations between $C_i(t)$ and $e^{-i\theta_i(t-\Delta t)}$, and so at large t and Δt it is expected to have the form

$$G^\theta(t, \Delta t) \sim e^{-M_\pi(t-\Delta t)} e^{-M_\rho \Delta t} \left(\alpha + \beta e^{-\delta M_\rho \Delta t} + ... \right), (2)$$

where $M_\rho + \delta M_\rho$ is the energy of the lowest-lying excited state of the ρ^+ leading to appreciable correlations between $C_i(t)$ and $e^{-i\theta_i(t-\Delta t)}$, and α and β are overlap factors that cannot be determined with general arguments but can be calculated with LQCD. The ellipses denote further-suppressed contributions from higher-lying states. A phase-reweighted effective mass can be defined as $M^\theta = \log\left(G^\theta(t, \Delta t)/G^\theta(t+1, \Delta t+1)\right)$, which
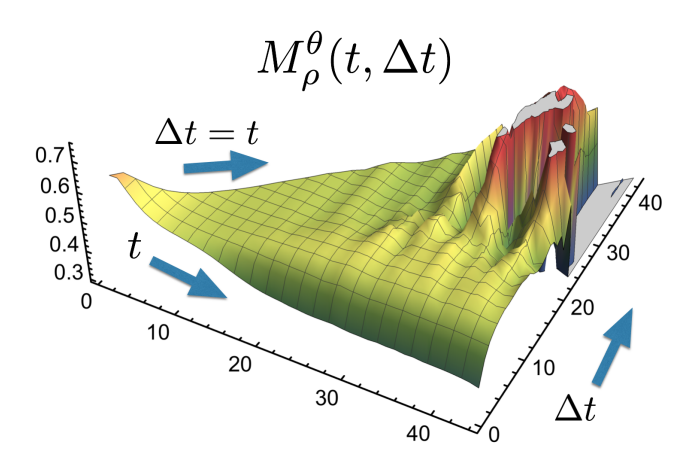
_____

[1] The phases of isovector meson correlation functions are restricted to be discrete values $\theta_\rho = 0$, π when interpolating operators in a Cartesian spin basis are used. In forthcoming work, we demonstrate that circular statistics applies to real but non-positive isovector meson correlation functions.
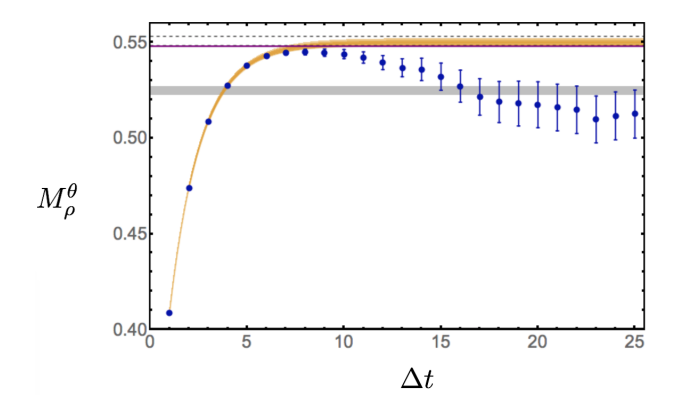

FIG. 3. The ρ^+ meson phase-reweighted effective mass for all $\Delta t \le t$. The standard effective mass in the upper panel of Fig. 2 corresponds to $M_\rho^\theta(t, t)$, a projection along the line $t = \Delta t$ indicated. The bottom panel of Fig. 2 shows $M_\rho^\theta(t, \Delta t)$ on lines of constant Δt parallel to the t axis indicated.

reduces to the standard effective mass definition when $\Delta t \to t$. For the ρ^+ meson, the form of the correlation function given in Eq. (2) leads to

$$M_\rho^\theta(t, \Delta t) = M_\rho + c \, \delta M_\rho e^{-\delta M_\rho \Delta t} + ... \, , \quad (3)$$

at large t, where $c = \beta/\alpha$ and the ellipses denote higher order contributions which are exponentially suppressed with Δt and standard excited state contributions that are exponentially suppressed with t.

LQCD calculations of M_ρ^θ summarized in Figs. 2-4 permit precise numerical study of small Δt bias and $\Delta t \to t$ extrapolation. These calculations employ $N \sim 130,000$ correlation functions previously computed by the NPLQCD collaboration from smeared sources and point sinks on an ensemble of 2889 isotropic-clover gauge-field configurations at a pion mass of $M_\pi \sim 450$ MeV generated jointly by the College of William and Mary/JLab lattice group and by the NPLQCD collaboration, see Ref. [32] for further details. The spacetime extent of the lattices is $48^3 \times 96$ at a lattice spacing of $a \sim 0.117(1)$ fm. For all of the correlation functions examined in this work, momentum projected blocks are derived from quark propagators originating from smeared sources localized about a site in the lattice volume, as detailed in previous works by the NPLQCD collaboration, e.g. Ref. [32, 33]. For instance, the blocks associated with the ρ^+ meson are

$$\mathcal{B}_\mu^{(\rho^+)}(\mathbf{p}, t; x_0) = \sum_{\mathbf{x}} e^{i\mathbf{p} \cdot \mathbf{x}} \, \overline{S}_d(\mathbf{x}, t; x_0) \gamma_\mu S_u(\mathbf{x}, t; x_0). (4)$$

Correlations functions are derived by contracting the blocks with local interpolating fields [34], e.g.,

$$C^{(\rho^+; \mu)}(\mathbf{p}, t; x_0) = \text{Tr}\left[\mathcal{B}_\mu^{(\rho^+)}(\mathbf{p}, t; x_0) \gamma^\mu \right], \quad (5)$$

FIG. 4. The ρ^+ mass extracted from late-time phase-reweighted correlation functions. The light-brown shaded region corresponds to the 68% confidence region associated with three-parameter (constant plus exponential) fits to Eq. (3). The dashed lines show the extrapolated M_ρ^θ result including statistical and systematic uncertainties described in the main text. The gray horizontal band corresponds to a determination of the ρ^+ mass from the plateau region [32]. The purple line corresponds to the $\pi\pi$ non-interacting p-wave energy.
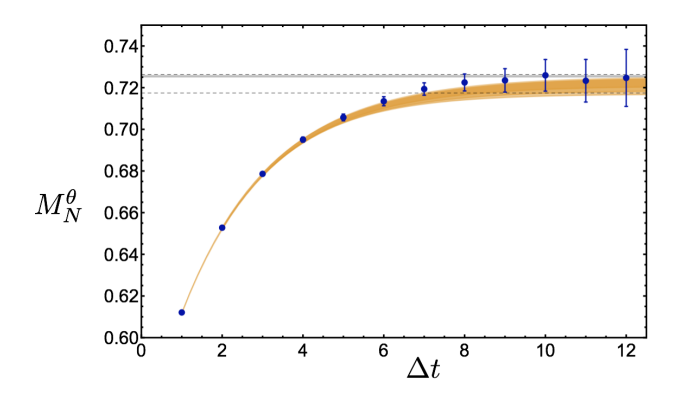

FIG. 5. The late-time nucleon phase-reweighted effective mass with statistical and systematic extrapolation errors shown with light-brown bands and dashed lines as in Fig. 4. The gray horizontal band corresponds to golden window result of Ref [32] obtained with four times higher statistics.

where the trace is over color and spin. It is the phases of contracted momentum-projected blocks that have been used to form phase-reweighted correlation functions. Expressions similar to those in eqs. (4) and (5) are used for the nucleon and two-nucleon systems [32, 33].

At large t and small Δt, bias in M_ρ^θ is consistent with Eq. 3. At intermediate Δt, M_ρ^θ approaches a value consistent with the $\pi\pi$ non-interacting p-wave energy $\sqrt{(2M_\pi)^2 + (2\pi/L)^2}$. At large Δt, M_ρ^θ approaches a lower-energy plateau consistent with the ρ^+ mass extracted from a $t = \Delta t$ plateau $t = 18 \to 28$. The suppression of ρ^+ bound state contributions compared to $\pi\pi$ scattering states contributions to $C_i(t)e^{-i\theta_i(t-\Delta t)}$ is found to be less severe in smaller volumes. The energy gap between the bound and scattering states also increases in smaller volumes. In accord with these arguments, the non-monotonic Δt behavior visible in Fig. 4 is not seen with $V = 32^3$ or $V = 24^3$. M_θ^ρ is consistent with the ρ^+ mass determined in Ref. [32] for $\Delta t \gtrsim 5$ in these smaller volumes. Variational methods employing phase reweighted correlation functions with multiple interpolating operators may be required to reliably distinguish closely spaced energy levels with large spatial volumes.

The nucleon mass does not appear to have complications from low-lying excited states and the late time phase-reweighted nucleon effective mass derived from $\sim 100,000$ sources with $V = 32^3$ [32] approaches its intermediate time plateau value at large Δt. Small Δt bias is well-described with a constant plus exponential form, and the nucleon excited state gap can be extracted across a range of fitting regions as $\delta M_N = 786(44)(25)$ MeV, where the first uncertainty is statistical from a correlated χ^2-minimization fit of $M_N^\theta(t, \Delta t)$ to Eq. (3) with

$\Delta t = 2 \to 10$ and $t = 30 \to 40$ and the second uncertainty is a systematic determined from the variation in central value when the fitting region is changed to be $\Delta t = 1 \to 10$ or $\Delta t = 3 \to 10$. This result is consistent with a naive extrapolation $M_\sigma \sim 830$ MeV of the σ-meson mass determined at $M_\pi \sim 391$ MeV [35]. Results for strange-baryon excited-state masses from phase-reweighted effective mass extrapolations are also consistent with the σ-meson mass in one- and two-baryon systems, for instance $\delta M_\Xi = 822(44)(71)$ MeV and $\delta M_{\Xi\Xi(^1S_0)} = 908(265)(82)$ MeV.

The $\Xi^-\Xi^-(^1S_0)$ has slower StN degradation than a two-nucleon system and is considered here for a first investigation of phase-reweighted baryon-baryon binding energies. The $\Xi^-\Xi^-(^1S_0)$ binding energy was determined by the NPLQCD collaboration to be $B_{\Xi\Xi(^1S_0)} = 15.4(1.0)(1.4)$ MeV for the gauge field configurations considered here using the correlation function production and sink-tuning [3–5] described for the deuteron and dineutron in Ref. [32].[2] Results for $\Xi^-\Xi^-(^1S_0)$ using the $\sim 100,000$ correlation function ensemble described above for constant fits to the phase reweighted binding energy with $t = 28 \to 43$, $\Delta t = 1, 2, 3 \to 6$ give $B_{\Xi\Xi(^1S_0)} = 15.8(3.5)(2.6)$ MeV. Consistency between golden window results and phase-reweighted results with large t and all $\Delta t \gtrsim 1$ suggests a high degree of cancellation at all Δt between excited state effects in one- and two-baryon phase reweighted effective masses. $B_{\Xi\Xi(^1S_0)}(t, \Delta t = 0)$, which only involves correlation function magnitudes, plateaus to $7.1(0.6)(0.8)$ MeV. Phase effects modify this magnitude result by an amount on the order of nuclear energy

---

[2] $B_{\Xi\Xi(^1S_0)} = -M_{\Xi\Xi(^1S_0)} + 2M_\Xi$ approaches the $\Xi\Xi(^1S_0)$ binding energy in the infinite volume limit. In finite volume $B_{\Xi\Xi(^1S_0)}$ differs from the infinite-volume binding energy by corrections that are exponentially suppressed by the binding momentum.
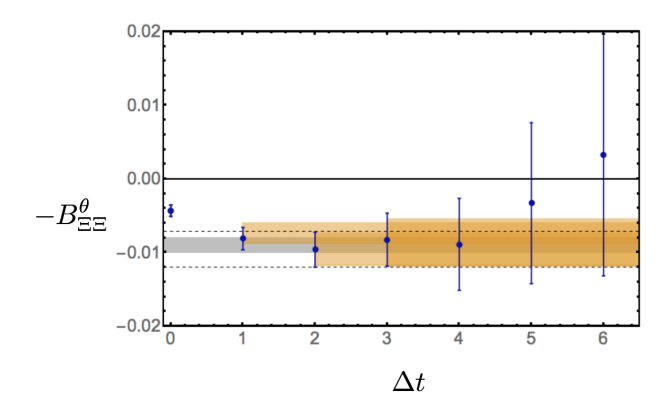
FIG. 6. The $\Xi^-\Xi^-(^1S_0)$ phase-reweighted binding energy with statistical and systematic extrapolation errors shown with light-brown bands and dashed lines as in Fig. 4. The gray horizontal band corresponds to the golden window result of Ref. [32], obtained with four times higher statistics.

scales rather than hadronic mass scales, providing encouraging evidence that extrapolations involving modest Δt can accurately determine nuclear binding energies in the noise region. The precision of phase-reweighted results scales with the number of points in the noise region, and could be increased on lattices of longer temporal extent then those used in this work (~ 11.2fm).

Phase reweighting allows energy levels to be extracted from LQCD correlation functions at times later than the golden window accessible to standard techniques involving source and sink optimization [3–5, 17, 18]. It is expected that these methods will permit the extraction of ground-state energies in systems without a golden window. The phase-reweighting method is equivalent to a dynamical source improvement in which the phase is held fixed while the magnitude of the hadronic correlation function is evolved into its ground state, and then the phase is released to provide a source for subsequent time slices. The bias introduced by phase reweighting can be removed by extrapolation but suffers from a StN problem that can be viewed as arising from evolution of the dynamically improved source. Generalizations of the phase-reweighting methods presented here may allow for reaction rates, operator matrix elements, and other observables to be extracted from phase-reweighted correlation functions.

---

[1] G. Parisi, *COMMON TRENDS IN PARTICLE AND CONDENSED MATTER PHYSICS. PROCEEDINGS, WINTER ADVANCED STUDY INSTITUTE, LES HOUCHES, FRANCE, FEBRUARY 23 - MARCH 11, 1983*, Phys. Rept. **103**, 203 (1984).

[2] G. P. Lepage, in *Boulder ASI 1989:97-120* (1989) pp. 97–120.

[3] S. R. Beane, W. Detmold, K. Orginos, and M. J. Savage, Prog. Part. Nucl. Phys. **66**, 1 (2011), arXiv:1004.2935 [hep-lat].

[4] S. R. Beane, W. Detmold, T. C. Luu, K. Orginos, A. Parreno, M. J. Savage, A. Torok, and A. Walker-Loud, Phys. Rev. **D79**, 114502 (2009), arXiv:0903.2990 [hep-lat].

[5] S. R. Beane, W. Detmold, T. C. Luu, K. Orginos, A. Par-

reno, M. J. Savage, A. Torok, and A. Walker-Loud, Phys. Rev. **D80**, 074501 (2009), arXiv:0905.0466 [hep-lat].

[6] M. G. Endres, D. B. Kaplan, J.-W. Lee, and A. N. Nicholson, Phys. Rev. Lett. **107**, 201601 (2011), arXiv:1106.0073 [hep-lat].

[7] M. G. Endres, D. B. Kaplan, J.-W. Lee, and A. N. Nicholson, Phys. Rev. **A84**, 043644 (2011), arXiv:1106.5725 [hep-lat].

[8] M. G. Endres, D. B. Kaplan, J.-W. Lee, and A. N. Nicholson, *Proceedings, 29th International Symposium on Lattice field theory (Lattice 2011): Squaw Valley, Lake Tahoe, USA, July 10-16, 2011*, PoS **LATTICE2011**, 017 (2011), arXiv:1112.4023 [hep-lat].

[9] J.-W. Lee, M. G. Endres, D. B. Kaplan, and A. N. Nicholson, *Proceedings, 29th International Symposium on Lattice field theory (Lattice 2011): Squaw Valley, Lake Tahoe, USA, July 10-16, 2011*, PoS **LATTICE2011**, 203 (2011), arXiv:1111.3793 [hep-lat].

[10] T. DeGrand, Phys. Rev. **D86**, 014512 (2012), arXiv:1204.4664 [hep-lat].

[11] D. Grabowska, D. B. Kaplan, and A. N. Nicholson, Phys. Rev. **D87**, 014504 (2013), arXiv:1208.5760 [hep-lat].

[12] A. N. Nicholson, D. Grabowska, and D. B. Kaplan, *Proceedings, Extreme QCD 2012 (XQCD12): Washington, USA, August 21-23, 2012*, (2012), 10.1088/1742-6596/432/1/012032, [J. Phys. Conf. Ser.432,012032(2013)], arXiv:1210.7250 [hep-lat].

[13] S. R. Beane, W. Detmold, K. Orginos, and M. J. Savage, J. Phys. **G42**, 034022 (2015), arXiv:1410.2937 [nucl-th].

[14] M. L. Wagman and M. J. Savage, (2016), arXiv:1611.07643 [hep-lat].

[15] S. R. Beane, E. Chang, S. D. Cohen, W. Detmold, H. W. Lin, T. C. Luu, K. Orginos, A. Parreno, M. J. Savage, and A. Walker-Loud (NPLQCD), Phys. Rev. **D87**, 034506 (2013), arXiv:1206.5219 [hep-lat].

[16] S. R. Beane *et al.* (NPLQCD), Phys. Rev. **C88**, 024003 (2013), arXiv:1301.5790 [hep-lat].

[17] W. Detmold and M. G. Endres, *Proceedings, 32nd International Symposium on Lattice Field Theory (Lattice 2014): Brookhaven, NY, USA, June 23-28, 2014*, PoS **LATTICE2014**, 170 (2015), arXiv:1409.5667 [hep-lat].

[18] W. Detmold and M. G. Endres, Phys. Rev. **D90**, 034503 (2014), arXiv:1404.6816 [hep-lat].

[19] C. Michael, Nucl. Phys. **B259**, 58 (1985).

[20] M. Lüscher and U. Wolff, Nucl. Phys. **B339**, 222 (1990).

[21] J. J. Dudek, R. G. Edwards, N. Mathur, and D. G. Richards, Phys. Rev. **D77**, 034501 (2008), arXiv:0707.4162 [hep-lat].

[22] B. Blossier, M. Della Morte, G. von Hippel, T. Mendes, and R. Sommer, JHEP **04**, 094 (2009), arXiv:0902.1265 [hep-lat].

[23] S. Zhang, J. Carlson, and J. E. Gubernatis, Phys. Rev. Lett. **74**, 3652 (1995).

[24] S. Zhang, J. Carlson, and J. E. Gubernatis, Phys. Rev. **B55**, 7464 (1997), arXiv:cond-mat/9607062 [cond-mat].

[25] R. B. Wiringa, S. C. Pieper, J. Carlson, and V. R. Pandharipande, Phys. Rev. **C62**, 014001 (2000), arXiv:nucl-th/0002022 [nucl-th].

[26] J. Carlson, S. Gandolfi, F. Pederiva, S. C. Pieper, R. Schiavilla, K. E. Schmidt, and R. B. Wiringa, Rev. Mod. Phys. **87**, 1067 (2015), arXiv:1412.3081 [nucl-th].

[27] D. B. Kaplan and M. J. Savage, Phys. Lett. **B365**, 244 (1996), arXiv:hep-ph/9509371 [hep-ph].

[28] T. A. Lähde, T. Luu, D. Lee, U.-G. Meißner, E. Epel-
baum, H. Krebs, and G. Rupak, Eur. Phys. J. **A51**, 92 (2015), arXiv:1502.06787 [nucl-th].

[29] M. Cè, L. Giusti, and S. Schaefer, Phys. Rev. **D93**, 094507 (2016), arXiv:1601.04587 [hep-lat].

[30] M. Cè, L. Giusti, and S. Schaefer, Phys. Rev. **D95**, 034503 (2017), arXiv:1609.02419 [hep-lat].

[31] M. Cè, L. Giusti, and S. Schaefer, *Proceedings, 34th International Symposium on Lattice Field Theory (Lattice 2016): Southampton, UK, July 24-30, 2016*, PoS **LATTICE2016**, 263 (2016), arXiv:1612.06424 [hep-lat].

[32] K. Orginos, A. Parreno, M. J. Savage, S. R. Beane, E. Chang, and W. Detmold, Phys. Rev. **D92**, 114512 (2015), arXiv:1508.07583 [hep-lat].

[33] S. R. Beane, P. F. Bedaque, K. Orginos, and M. J. Savage, Phys. Rev. Lett. **97**, 012001 (2006), arXiv:hep-lat/0602010 [hep-lat].

[34] W. Detmold and K. Orginos, Phys. Rev. **D87**, 114512 (2013), arXiv:1207.1452 [hep-lat].

[35] R. A. Briceño, J. J. Dudek, R. G. Edwards, and D. J. Wilson, Phys. Rev. Lett. **118**, 022002 (2017), arXiv:1607.05900 [hep-ph].

[36] R. G. Edwards and B. Joo (SciDAC Collaboration, LHPC Collaboration, UKQCD Collaboration), Nucl.Phys.Proc.Suppl. **140**, 832 (2005), arXiv:hep-lat/0409003 [hep-lat].

Supplemental Material

Δt	$M_{\rho^+}^{\theta}$	M_N^{θ}	$B_{\Xi\Xi(^1S_0)}$
1	0.40872(21)	0.61209(50)	-0.0081(15)
2	0.47392(30)	0.65278(66)	-0.0096(24)
3	0.50841(40)	0.67861(88)	-0.0083(36)
4	0.52722(52)	0.6951(12)	-0.0089(62)
5	0.53774(67)	0.7057(16)	-0.003(11)
6	0.54284(84)	0.7135(22)	0.003(16)
7	0.5446(11)	0.7193(30)	-
8	0.5449(15)	0.7225(41)	-
9	0.5446(19)	0.7235(56)	-
10	0.5439(23)	0.7259(76)	-
11	0.5421(30)	0.723(10)	-
12	0.5395(37)	0.725(14)	-
13	0.5368(47)	-	-
14	0.5359(58)	-	-
15	0.5321(71)	-	-
16	0.5271(83)	-	-
17	0.5215(95)	-	-
18	0.519(11)	-	-
19	0.518(12)	-	-
20	0.517(12)	-	-
21	0.516(12)	-	-
22	0.515(12)	-	-
23	0.510(12)	-	-
24	0.512(13)	-	-
25	0.513(13)	-	-
PR Ground	0.5222(60)(27)	0.7220(33)(11)	-0.0096(22)(11)
PR Excited	0.5508(11)(7)	-	-
GW Ground	0.5248(14)(15)	0.72551(35)(26)	-0.00909(59)(83)
GW $\pi\pi$	0.547997(78)(14)	-	-

TABLE I. Phase-reweighted (PR) effective masses of the ρ^+, nucleon and the effective energy difference between $\Xi\Xi(^1S_0)$ and two Ξ's derived from eq. (1). The extrapolated PR ground values are taken from three-parameter constant plus exponential correlated χ^2-minimization fits for M_N^{θ} and one-parameter constant fits for $B_{\Xi\Xi(^1S_0)}^{\theta}$ with statistical uncertainties for fits starting at $\Delta t = 2$ and systematic uncertainties defined from variation of the Δt fitting window as described in the main text. PR data is taken from $t = 28 \to 43$ for the ρ^+ and $\Xi\Xi(^1S_0)$ and $t = 31 \to 40$ for the nucleon. For the ρ^+, the region $\Delta t = 2 \to 10$ is used to constrain the first scattering state for the PR excited state result, while the region $\Delta t = 16 \to 25$ is used to constrain the ground state. Golden window (GW) ground refers to the ground-state energy determinations using the short and intermediate time plateau regions described in Ref. [32]. GW $\pi\pi$ refers to the non-interacting p-wave energy shift $\sqrt{(2M_\pi)^2 + (2\pi/L)^2}$ using M_π and L for the 48^3 ensemble described in the main text.